DOI: 10.12442/j.issn.1002-185X.20240781

Effect of grain refinement on grain boundary diffusion process and magnetic properties of sintered NdFeB magnets

Wang Mei [1], Liu Weiming [2], Peng Buzhuang [3], Wang Qian [1,*], Wang Fei [1], Zhang Yumeng [3], Gu Xiaoqian [3], Wang Qi [1], Xiao Guiyong[1], Liu Yan[3] and Zhu Xinde [1,4,*]

[1]Key Laboratory for Liquid-Solid Structural Evolution and Processing of Materials (Ministry of Education), Shandong University, Jinan 250061, P.R. China; [2]Yantai Standard and Metrology Inspection and Testing Center, Yantai 264000, P.R. China; [3]Yantai Zhenghai Magnetic Material Co., Ltd., Yantai 264006, P.R. China;[4]Jianxin Zhao's Group Co. Ltd., Ningbo 315600,P.R. China;

Abstract: Three types of NdFeB magnets of the same composition and different grain sizes were prepared, and then the grain boundary diffusion was carried out using metal Tb under the same technical parameters. The effect of grain size on the grain boundary diffusion process and properties of sintered NdFeB magnets was investigated. The diffusion course was assessed using X-ray diffraction (XRD), field emission scanning electron microscope (FESEM) and electron probe microanalyzer (EPMA). The magnetic properties of the magnet before and after diffusion were investigated. The results show that the grain refinement of the magnet leads to higher Tb utilization efficiency and results in higher coercivity at different temperatures, which can be attributed to the formation of a deeper and more complete core-shell structure, resulting in better magnetic isolation and higher anisotropy of the $Nd_2Fe_{14}B$ grains. This work may shed light on developing high coercivity with low heavy rare earth through grain refinement.

Keywords*:* sintered NdFeB magnets; grain refinement; grain boundary diffusion; coercivity

1. Introduction

Sintered NdFeB magnets are widely used in hard disk drives, new energy vehicles, wind power generation[1], industrial permanent magnet motors, consumer electronic devices, and magnetic medical devices[2] because of their excellent magnetic properties. In recent years, the rapid development of the high-end application market of magnets has promoted innovation in the fabrication techniques of NdFeB magnets, especially the long-term service of magnets at high operating temperatures[3]. Intrinsic coercivity is an important indicator of NdFeB magnets to resist thermal demagnetization, and NdFeB magnets should theoretically have high coercivity to withstand demagnetization at high operating temperatures[4].

Grain boundary diffusion technology is to diffuse heavy rare earth elements into permanent magnets through grain boundary phases under high temperature vacuum conditions[5-6], which is a major technological innovation in the sintered NdFeB permanent magnet industry in the 21st century. It achieves high coercivity and high

Foundation item: Key Research and Development Program of Shandong Province (2021CXGC010310); Shandong Province Science and Technology Small and Medium sized Enterprise Innovation Ability Enhancement Project (2023TSGC0287 and 2024TSGC0519); Shandong Provincial Natural Science Foundation (ZR2022ME222), National Natural Science Foundation of China (51702187).

*Corresponding author: Zhu Xinde, Ph. D., Key Laboratory for Liquid-Solid Structural Evolution and Processing of Materials (Ministry of Education), Shandong University, Jinan 250061, P.R.China and Jianxin Zhao's Group Co. Ltd., Ningbo 315600, P.R.China, Email: zhuxinde@sdu.edu.cn;

Wang Qian, Ph. D., Key Laboratory for Liquid-Solid Structural Evolution and Processing of Materials (Ministry of Education), Shandong University, Jinan 250061, P.R.China, Email: qian.wang@sdu.edu.cn

magnetic energy product while significantly reducing the use of heavy rare earth elements[7]. For grain boundary diffusion technology, the research and development of high-efficiency and low-cost diffusion agents has always been the focus of research. According to the composition of the diffusion agent, it can be divided into three categories. The first type of diffusion agent are mainly pure metals, alloys and compounds of heavy rare earth elements (Tb and Dy)[8]. During diffusion, Tb/Dy first diffuses along the grain boundary phase and then substitutes Nd in the $Nd_2Fe_{14}B$ lattice. As a result, a core-shell type microstructure is obtained as the Tb/Dy diffused into $Nd_2Fe_{14}B$ forms a $(Nd,Tb/Dy)_2Fe_{14}B$ shell, which magnetically hardens the whole magnet[8]. And consequently, the coercivity of the magnet is greatly improved without or slightly decreasing in remanence, while reducing the use of heavy rare earths. The second type of diffusion agent is light rare earth elements, including Nd-Al[9], Pr-Cu[10] and Pr-Al-Cu[11]. This diffusion agent can mainly increase the amount and thickness of non-magnetic grain boundary layers between grains, better isolate the magnetic coupling between grains, and thus increase the coercivity of the magnet. The third type of diffusion agent is non-rare earth-based compounds, metals and alloys[12–15], which works the same way as the second type of diffusion agent.

So far, the most effective diffusion agent for improving coercivity is still the first type, however, the production of large quantities of high coercivity NdFeB magnets containing Dy/Tb faces cost and raw material supply difficulties[8–15]. Therefore, it has become a major issue to reduce the strong dependence of high coercivity NdFeB magnets on heavy rare earths and realize the high efficiency utilization of rare earth resource. H. Sepehri-Amin[16] investigated the grain size dependence of coercivity in NdFeB sintered magnets by finite-element micromagnetic simulations, and attributed the increase in coercivity with a decrease in grain size to the reduction in stray field arising from neighboring grains. Experimental studies[17–19] also have shown that the coercivity of NdFeB magnets increases with decreasing of grain size. However, the coercivity of the sintered magnet is significantly reduced when the grain size is reduced below the critical size (about 3 μm). This is mainly due to the fact that ultrafine powders are easily oxidized in the process of powder metallurgy[20].

By taking advantage of the enhancing effect of grain boundary diffusion and grain refinement on coercivity, it is possible to reduce the amount of heavy rare earths and obtain a higher coercivity at the same time. However, there are few relevant studies on the influence of microstructure changes of matrix materials on the grain boundary diffusion process[21–24], and the mechanism of grain refinement on coercivity has not been studied in detail. In order to understand the effect of grain size on diffusion process and coercivity enhancement, it is necessary to systematically study the microstructure and composition distribution of magnets with different grain sizes after grain boundary diffusion. In this paper, non-heavy rare earth matrix magnets with the same composition and different grain sizes were selected as the original magnets, and the changes in microstructure and magnetic properties before and after Tb diffusion were observed through the same diffusion process, so as to find out the internal relationship between grain size and the change in properties after grain boundary diffusion.

2. Material and methods

Three types of NdFeB magnets (named S0, S1 and S2) with different grain sizes were fabricated by fully automatic scale casting, hydrogenation powder production, automatic molding, continuous sintering at 1050 °C, and subsequent twice tempering (at 900 °C and 500 °C for 5 h) in a mixture of N_2, Ar, and H_2 (the base pressure was < 10^{-3} Pa), which is called an oxygen-free process technology[25]. Grain size was varied by changing the particle size of jet-milled powders. The obtained NdFeB magnets were selected as the original magnets for Tb diffusion. In order to avoid the influence of rare earth content changes and other process variables on the final analysis results, the three types of samples in this study had the same composition and preparation process parameters except for the different process parameters in the jet milling and milling stages, and the subsequent Tb grain boundary diffusion technical parameters were also the same. A self-developed three-dimensional magnetron sputtering apparatus was used to deposit Tb metal film (the weight gain ratio of Tb metal is 0.8%) to the surface of the magnets at room temperature using metallic Tb (purity: > 99.9%) as a diffusion source, and

then grain boundary diffusion was conducted in a high vacuum condition at 900 ºC for 10 h, followed by annealing at 500 ºC for 2 h. The corresponding magnets after Tb diffusion named as S0 diff., S1 diff. and S2 diff.

The average particle size of the jet-milled powder was measured by a laser particle size analyzer and the corresponding grain size of the sintered magnet (corroded with alcohol and nitric acid) was analyzed by a scanning electron microscope (Fig. 1). The main composition design, particle size and the average grain size of the three types of magnets are shown in Table 1. The magnetic properties of the magnets before and after diffusion were tested at 20 ºC, 90 ºC, 140 ºC by NIM-10000H hysteresigraph, respectively. The surface phase of the magnets before and after diffusion was studied using DMAX-2500P X-ray diffraction (XRD) with Cu K-beta radiation. JSM-7800F field emission scanning electron microscope (FESEM) was performed for the microstructure observation. The area distribution of the main elements was determined by JXA-8530F Plus electron probe microanalyzer (EPMA).

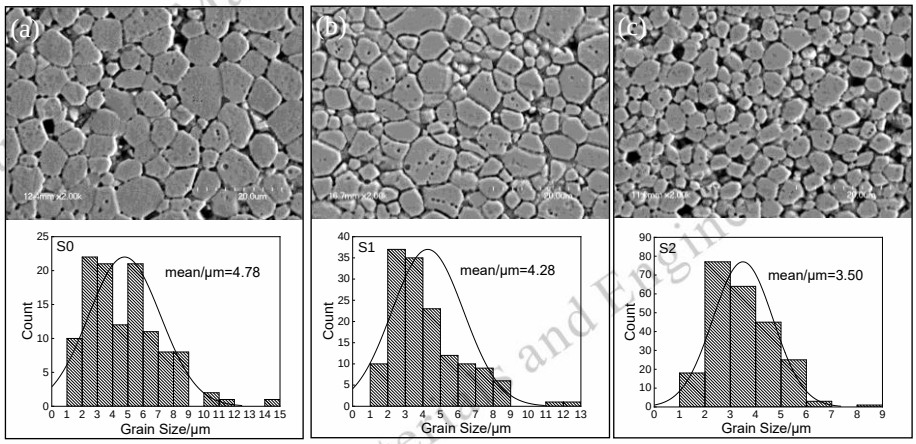

Fig.1 SEM images of the S0 (a) S1 (b) and S2 (c) magnets and the corresponding grain size distributions.

Table 1

Composition (%, mass fraction), particle size and grain size of the original samples (S0, S1, S2).

Sample	Composition (%)	Particle size (VMD)(μm)	Grain size (μm)
S0	$Nd_{28.5}Ho_{2.5}Fe_{65.1}B_{1.0}$	5.6	4.78
S1	$Nd_{28.5}Ho_{2.5}Fe_{65.1}B_{1.0}$	4.8	4.28
S2	$Nd_{28.5}Ho_{2.5}Fe_{65.1}B_{1.0}$	3.9	3.50

3. Experimetal results

3.1. Grain size and magnetic properties

Fig. 2 shows the backscatter electron (BSE) SEM images of S0 diff., S1 diff. and S2 diff. and the corresponding grain size distributions, which were calibrated using the diameter of equal area circle of the main grains in Fig. 2(a), (b) and (c) by Image J. It can be found that the average grain sizes of S0 diff., S1 diff. and S2 diff. magnets, which fabricated by jet-milled powders with different average particle sizes (as shown in Table 1), are 4.22 μm, 4.06 μm, 3.47 μm, respectively. Compared to sintered NdFeB magnets (S0, S1, S2) (as shown in Fig.1), the main grain size decreased slightly after diffusion, which can be attributed to the formation of a Tb-rich shell structure, and the details will be discussed in section 3.2.

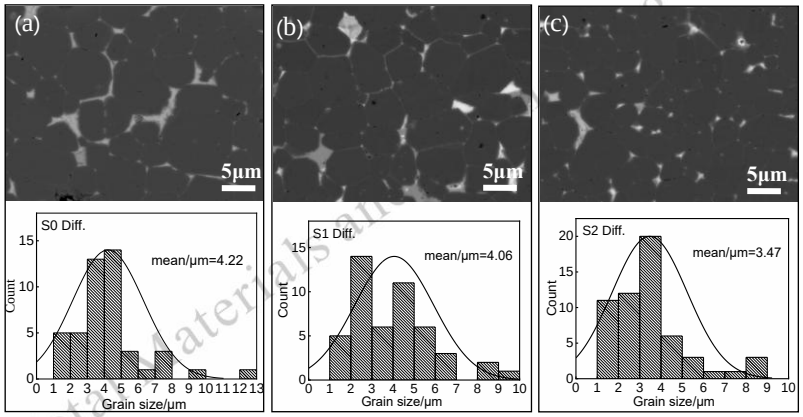

Fig.2 Backscattered electron SEM images of the S0 diff. (a) S1 diff. (b) and S2 diff. (c) magnet at a diffusion depth of 300 μm and the corresponding grain size distributions.

Fig. 3 demonstrates the demagnetization curves of three types of magnets before and after diffusion at 20 ºC. The magnetic properties of the magnets are listed in Table 2. Compared to the original magnets, the coercivity of S0 diff. increased from 11.83 kOe to 25.42 kOe, S1 diff. increased from 12.54 kOe to 26.61 kOe, while S2 diff. increased from 12.78 kOe to 27.06 kOe at the same Tb weight gain ratio. It is evident that S2 diff. magnets exhibit the highest coercivity and the highest coercivity increments compared to S0 diff. and S1 diff. magnets, as shown in Fig. 3(a), which demonstrates the advantage of the grain refinement in improving coercivity.

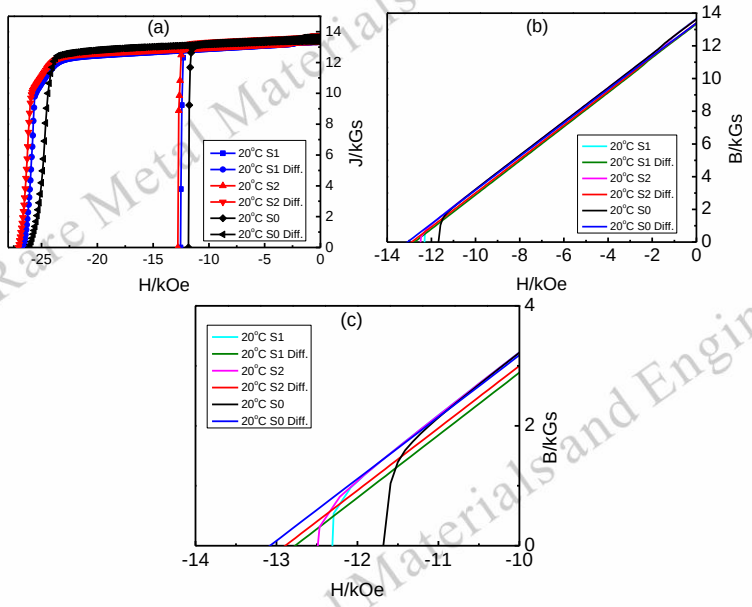

Fig. 3 Demagnetization J–H (a) and B–H (b) curves of the magnets (S0, S1 and S2) before and after Tb diffusion at 20 ºC.

Table 2

Magnetic properties at different temperatures of the magnets before and after Tb diffusion.

Sample	Temperature (ºC)	Br (kGs)	Hcj (kOe)	(BH)max (MGOe)
S0	20	13.63	11.83	44.53

S1	20	13.66	12.54	44.50
S2	20	13.65	12.78	44.54
S0 Diff.	20	13.39	25.42	41.84
	90	12.68	16.42	36.86
	140	11.70	10.95	31.21
S1 Diff.	20	13.34	26.61	42.47
	90	12.55	17.34	37.05
	140	11.68	11.69	31.84
S2 Diff.	20	13.40	27.06	43.09
	90	12.46	17.52	37.14
	140	11.67	12.32	32.19

The linear B–H curve is a very important characteristic that enables the magnets to be stable during operation. Under ideal conditions, it should be a straight line with a slope of 1. Fig. 3 (b) depicts magnet remanence (Br) variations of the S0, S1 and S2 magnets before and after Tb diffusion at 20 °C, reflecting the maximum magnetic energy product (BHmax) of the magnets. The B–H curves of the S0 diff., S1 diff. and S2 diff. magnets (blue line, red line and green line) show a straight line, while the curves of the original magnets show a knee-like characteristic when the residual magnetism approaches zero. This indicates that the microstructure and density of the magnets are improved after Tb diffusion[8]. As shown in Table 2, the corresponding maximum magnetic energy products of S0, S1 and S2 after Tb diffustion at 20 °C had values of 41.84, 42.47 and 43.09 MGOe, representing decreases of 6.0%, 4.6% and 3.3% after diffusion. It can be seen that magnet grain refinement can weaken the magnetism reduction caused by Tb diffusion.

Fig. 4 shows the demagnetization J–H (a) and B–H (b) curves of the magnets after Tb diffusion at 20 °C, 90 °C and 140 °C. The magnetic properties of the magnets are listed in Table 2. It can be found that both the coercivity and remanence of the S0 diff., S1 diff. and S2 diff. magnets all decrease with increasing temperature, but the S2 diff. magnet possesses the highest coercivity compared to the S0 diff. and S1 diff. magnets at 20 °C, 90 °C, and 140 °C, and the corresponding maximum magnetic energy product of S2 diff. magnet is also slightly higher than that of the S0 diff. and S1 diff. magnets.

Based on the above results, it can be inferred that the grain refinement of the magnet leads to higher coercivity at different temperatures. The same phenomenon is observed in the Dy diffusion experiment[21].

3.2. Microstructure and elemental distribution

Since the coercivity of NdFeB permanent magnets is extremely sensitive to their microstructure, especially the grain boundary structure and chemistry composition, the phase structure, microstructure and elemental distribution of the magnets were systematically studied by XRD, FESEM and EPMA measurements.

The XRD diffraction patterns of the six types of samples (S0, S1, S2, S0 diff., S1 diff. and S2 diff.) are shown in Fig. 5. As can be seen from the Fig. 5 (a), the main diffraction peaks of six samples are almost identical, mainly (004), (105), (006), etc., all of which are characteristic peaks of the $Nd_2Fe_{14}B$ phase, which is the magnetic source of the magnet. It is found in both diffused and original magnets that the intensity value of (006) is higher than that of (105), which demonstrats that the c-axis orientation of the magnets was substantially preserved after diffusion, showing all the magnets have good orientation. All characteristic peaks of the original S0 sample are positioned at lower angles than those of original S1, S2 samples and all of their characteristic peaks of $Nd_2Fe_{14}B$ matrix phases shift slightly toward a higher angle after Tb diffusion indicating a reduction in crystal plane spacing (as shown in Fig. 5 (b) and (c)), which can be attributed to the formation of $(Nd,Tb)_2Fe_{14}B$ [26].

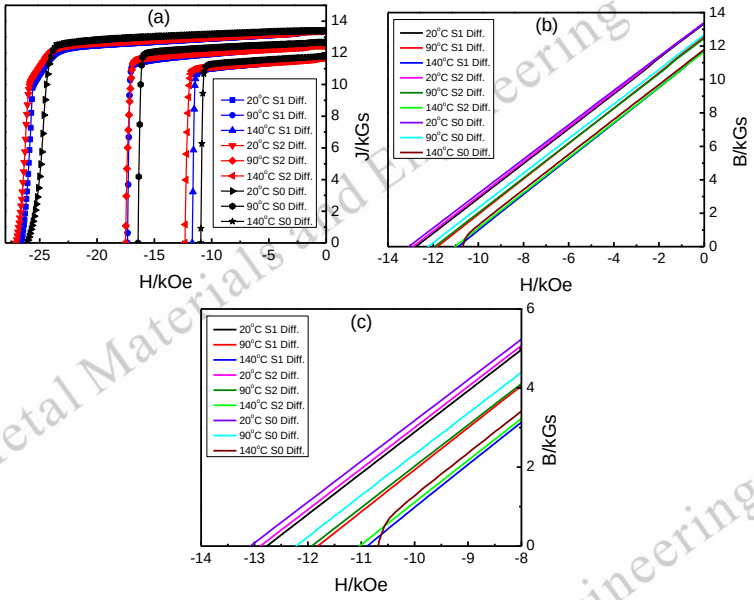

Fig. 4 Demagnetization J–H (a), B–H (b) and local magnification of B–H (c) curves of the magnets after Tb diffusion at 20 ºC, 90 ºC and 140 ºC.

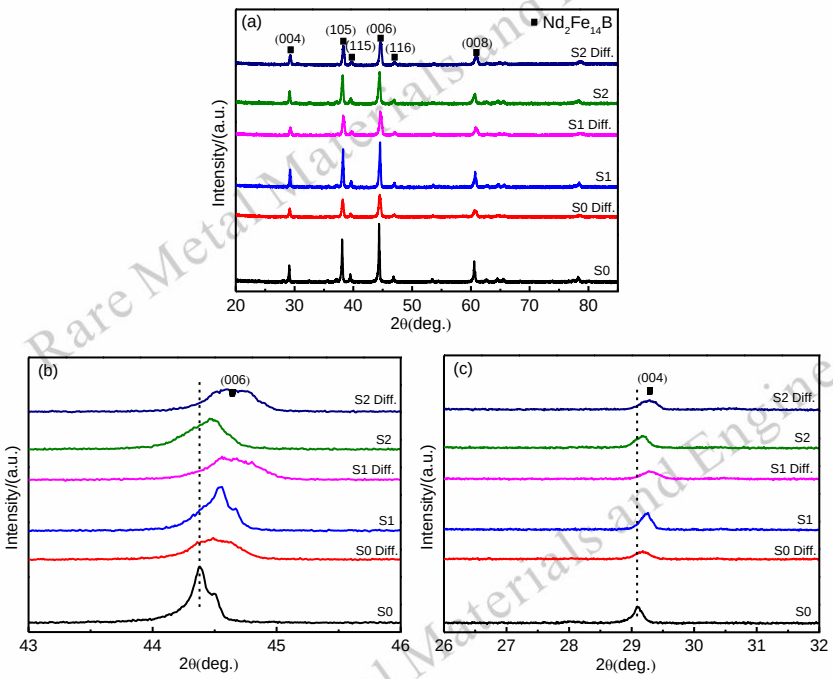

Fig. 5 (a) XRD diffraction patterns of S0, S1, S2, S0 diff., S1 diff. and S2 diff. magnets; the characteristic peaks (b) (006) and (c) (004) partial enlarged.

Backscattered images of the magnets before and after Tb diffusion (diffusion depths: 50 μm, 300 μm and 2750 μm) are shown in Fig. 6. As is known that bright contrast corresponds to phases containing more rare earth

elements. The grain boundary of the S1 diff. magnet (Fig. 6 (b1, b2)) is much clearer than that of the S0 diff. and S2 diff. magnets (Fig. 6 (a1, a2) and Fig. 6 (c1, c2)) at the diffusion depths of 50 μm and 300 μm, indicating a thicker Nd-rich phase exists in the S1 diff. magnet.

It can be seen from Fig. 6(a1, b1, c1) that after Tb diffusion, there formed a bright gray shell in the outer region of the $Nd_2Fe_{14}B$ grains in S0 diff., S1 diff. and S2 diff. magnets at a depth of 50 μm, and the shell thickness around the main grains of S0 diff., S1 diff. and S2 diff. magnets is 0.6~1.8 μm, 0.6~1.2 μm, and 0.3~0.6 μm, respectively. The shell structure of the S2 diff. magnet is not only thinner but more uniform compared to that of the S0 diff. and S1 diff. magnets. It has been reported that the shell structure is caused by the diffusion of Tb into the $Nd_2Fe_{14}B$ phase and the formation of $(Nd,Tb)_2Fe_{14}B$ shell around main grains[8,17]. Furthermore, at a diffusion depth of 300 μm, a thinner shell than that located at the diffusion depth of 50 μm can be found in the S2 diff. magnet (marked by red arrows in Fig.6 (c2)), while no obvious core-shell structure could be observed in the S1 diff. magnet which can be attribute to the lower Tb content. This indicates that the fine-grained magnet facilitates the diffusion of Tb into the magnets, resulting in a deeper and clearer shell structure. It demonstrates a higher Tb utilization efficiency in the S2 diffusion process. The core-shell structure can not be found at the center of all the magnets (the depth is 2750 μm), showing the content of Tb in the center of three magnets all is low.

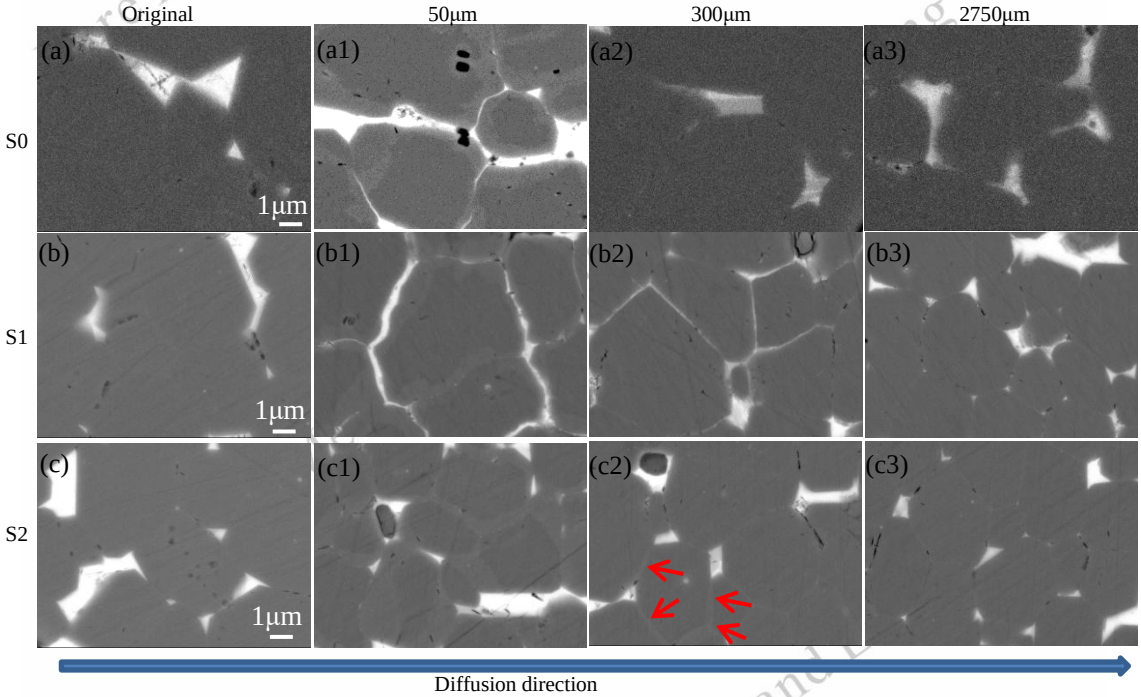

Fig. 6 Backscattered electron SEM images of the S0 (a), S1 (b), S2 (c) magnets and S0 diff.(a1,a2,a3), S1 diff. (b1,b2,b3) and S2 diff. (c1,c2,c3) magnets at different diffusion depths (a1) (b1) (c1): 50 μm, (a2) (b2) (c2): 300 μm, (a3) (b3) (c3): 2750 μm (center).

Fig. 7 depicts the EPMA images of the cross-section of S1 diff. and S2 diff. magnets at 0~300 μm depth. The results reveal that the Tb distribution of S2 diff. magnet is more uniform and dispersed from the surface to the depth of 300 μm in comparison to that of the S0 diff. and S1 diff. magnets. There are more Tb elements concentrated near the surface of the the S0 diff. and S1 diff. magnets than that of the S2 diff. magnet at the same Tb weight gain ratio, indicating the Tb diffusion in the S2 diff. magnet is relatively more sufficient. The distribution of Nd in the S2 diff. magnet is homogeneous, whereas many Nd element gatherings can be observed in the S0 diff. and S1 diff. magnet. In addition, Nd enrichment decrease near the surface of the magnets can be clearly observed in three types of magnets as shown by rectangle in red colour (Fig. 7 (a2, b2, c2)). The reduction

of the Nd enrichment was attributed to the diffusion of Nd element from the magnet to the coating layer because the Nd-rich liquid phase was present during the diffusion process at 900 °C[27].

To investigate the detailed distribution of Tb and Nd elements in the magnets after diffusion, the element distribution of S0 diff. (Fig. 8 (a1, a2, a3)) , S1 diff. (Fig. 8 (b1, b2, b3)) and S2 diff. magnets (Fig. 8 (c1, c2, c3)) at diffusion depths of 100 μm and 300 μm were analyzed repectively using EPMA. Thicker Nd-rich phase along the grain boundary can be observed in the Nd map of S1 diff. magnet compared to the S0 diff. and S2 diff. magnet. This is consistent with the results in Fig. 6.

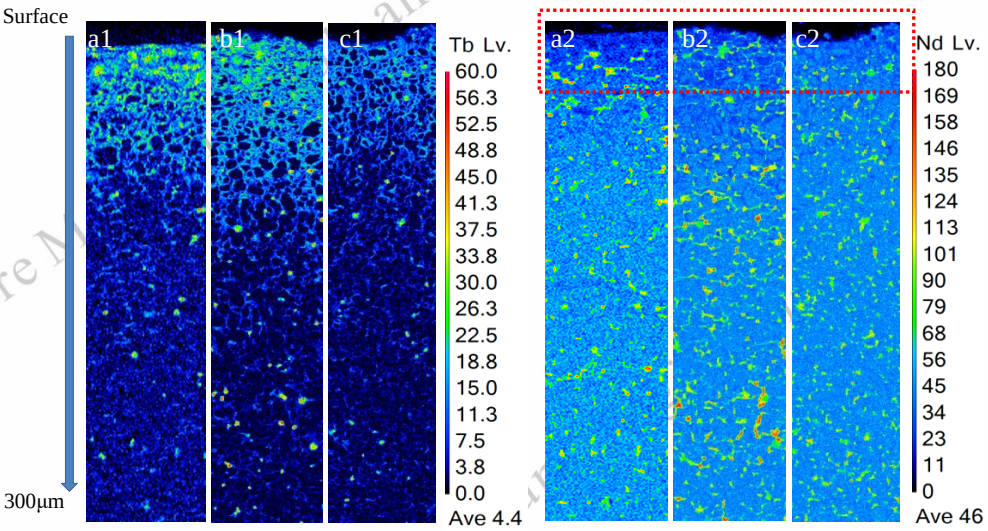

Fig. 7 Cross sectional EPMA images of S0 diff. (a1, a2), S1 diff. (b1, b2) and S2 diff. (c1, c2) magnets at 0~300 μm.

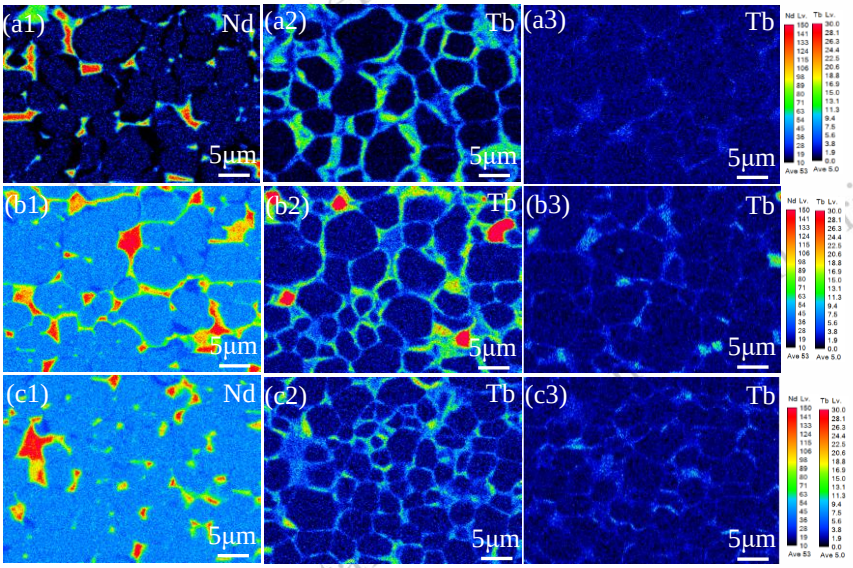

Fig. 8 EPMA element scan images of S0 diff.(a1, a2, a3), S1 diff. (b1, b2, b3) and S2 diff. (c1, c2, c3) magnets at different diffusion depths:(a1) (a2) (b1)(b2)(c1)(c2): 100 μm, (a3) (b3) (c3): 300 μm.

By comparing the backscatter pattern in Fig.2 and the EPMA pattern in Fig. 8, it can be seen that the Tb enrichment zone corresponds exactly to the grain boundary position of the magnets, which proves that the

diffused Tb element is mainly distributed in the grain boundary position of the magnets. As shown in Fig. 6 (b1, c1, c2), a core-shell structure is obtained as the Tb element diffused into the $Nd_2Fe_{14}B$ forms a $(Nd,Tb)_2Fe_{14}B$ shell. Here, a well-connected network Tb-rich shell around $Nd_2Fe_{14}B$ grains can be easily found in S0 diff., S1 diff. and S2 diff. magnets at diffusion depth of 100 μm. Furthermore, compared with S2 diff. magnet (Fig. 8 (c2)), higher Tb enrichment and higher areal fraction of the triple junction phase can be observed in S0 diff. and S1 diff. (Fig. 8 (a)) at the same Tb weight gain ratio. However, at diffusion depth of 300 μm, the "well-connected network" Tb enrichment still can be observed in S2 diff. magnet (Fig. 8 (c3)), while S0 diff. magnet shows the least continuous Tb enrichment along the grain boundary (Fig. 8 (a3)). It can be infered that the Tb distribution in S2 diff. magnet is fairly homogeneous and continuous, confirming that the Tb diffusion in S2 diff. magnet is more sufficient than that in S0 diff. and S1 diff. magnet. This is consistent with the results in Fig. 6.

4. Discussion

Fig. 8 displays the schematic diagram of grain boundary diffusion for coarse-grained (Fig. 9 (a)) and fine-grained (Fig. 9 (b)) magnets. As shown in the schematic diagram, the number of magnet grain boundaries is increased due to grain refinement, which increases the diffusion channels of Tb element. In other words, grain refinement will lead to increased diffusion depth along the grain boundary in the magnet, so the diffusion efficiency of Tb in fine-grained magnet is better than that in coarse-grained magnets. This is consistent with the results observed in Fig. 6 and Fig. 8. A similar situation has been reported in a previous report[28]. In addition, due to the refinement of the main phase grains, more grain boundary layers are formed, fine-grained magnets have higher defect densities and greater grain boundary distortion energies, which provide a greater driving force for element diffusion[6]. And the atoms in the boundary layer are in a high energy state, after thermal activation, it is extremely easy to undergo atomic transitions and form vacancies, promoting the diffusion of heavy rare earth elements along the interface of the grain boundary layer. It is equivalent to the "auxiliary path" of the grain boundary layer as an element diffusion channel, which expands the diffusion path of the element. Moreover, these "auxiliary paths" are continuous and almost fault-free[28-29]. Therefore, the diffusion of heavy rare earths in fine-grain magnets is more uniform and more sufficient than that in coarse-grained magnets.

The diffusion of heavy rare earth elements in the magnet is not only along the grain boundaries to the interior of the magnet, but also from the grain boundaries to the interior of the main phase grains. The higher the concentration of heavy rare earth elements at the grain boundaries, the more heavy rare earth elements diffuse into the main phase grains through the body, resulting in the formation of a thicker shell structure on the periphery of the main phase grains. In coarse-grained magnets, the concentration of Tb near the surface (at diffusion depths of 50μm and 100 μm) is higher, the diffusion of heavy rare earths to the main phase grains is stronger, and the shell structure of $(Nd,Tb)_2Fe_{14}B$ is thicker (as shown in Fig. 6 and Fig. 8). However, the concentration of Tb close to the sample center is higher in fine-grained magnets and a clearer shell structure can be observed at a diffusion depth of 300 μm (as shown in Fig. 6 and Fig. 8).

After grain boundary diffusion, the coercivity of magnets increased due to two main factors. First, the formation of a core-shell structure enhances the magnetocrystalline anisotropy field of the defect layer on the grain surface. Nevertheless, if the shell structure is too thick, it will cause the waste of heavy rare earth elements in the diffusion process, and will also lead to the decline of magnet remanence. Secondly, the increased grain boundary phase results in a better magnetic isolation effect among grains. Therefore, the difference in the concentration distribution of heavy rare earths in magnets with different grain sizes results in differences in coercivity.

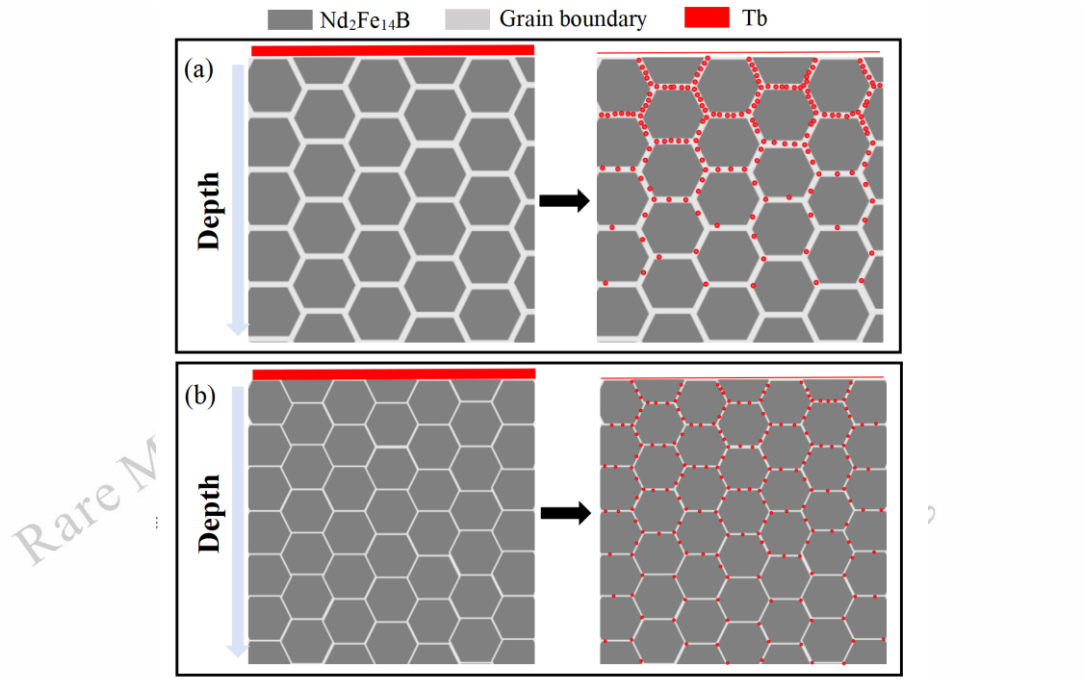

Fig. 9 The schematic diagram of grain boundary diffusion for different grain size ((a) coarse-grained (b) fine-grained) magnets.

The S2 diff. magnet exhibits a deeper and more complete core-shell structure when compared to the S0 diff. and S1 diff. magnet, resulting in a better magnetic isolation and higher-anisotropy of the $Nd_2Fe_{14}B$ grains with the formation of the Tb-rich shell. However, the S1 diff. magnet shows thicker Nd-rich phase along grain boundaries, which can better wrap the $Nd_2Fe_{14}B$ grains and strengthen the demagnetization coupling effect. As discussed in Section 3.1, the S2 diff. magnet possesses a higher coercivity than the S1 diff. magnet. It can be considered that the shell structure formed by the Tb substitution is the main factor of the coercivity enhancement in the grain boundary diffusion process. The deeper diffusion depth of heavy rare earth elements makes the distribution of Tb in the magnet more uniform, and the distribution of Tb elements in the deep shell structure is higher, which is the reason for the greater increase in coercivity after the diffusion of magnets with finer grains. In addition, as shown in Table 2, most of the magnetic properties of S2 diff. magnets are better than those of S0 diff. and S1 diff. magnets, which can be attributed to the more homogeneous and deeper distribution of Tb, resulting in less antiferromagnetic coupling between Tb and Fe.

5. Conclusion

NdFeB magnets with different grain sizes and the same composition were prepared, and then grain boundary diffusion was carried out using metal Tb under the same technical parameters. The formation of a deeper and more complete core-shell structure in the fine-grained (S2 diff.) magnets demonstrates that the grain refinement could allow more Tb to diffuse deep into the magnet, resulting in better magnetic isolation and higher-anisotropy of the $Nd_2Fe_{14}B$ grains. However, the coarse-grained (S1 diff.) magnet shows a thicker Nd-rich phase than that of the fine-grained magnet, which can better wrap the $(Nd)_2Fe_{14}B$ grains and strengthen the demagnetization coupling effect. Even so, the results show that the fine-grained magnet displays higher coercivity at different temperatures compared with the coarse-grained magnet. It can be considered that the core-shell structure formed by the Tb substitution is the main factor of the coercivity enhancement in the grain boundary diffusion process.

Thus, the grain size of the original magnets can affect the grain boundary diffusion process and determine the microstructure and coercivity.

References

1. Li L, Post B, Kunc V, Elliott AM, Parans M. Additive manufacturing of near-net-shape bonded magnets: prospects and challenges. *Scri. Mater.*[J], 2017, 135: 100.
2. Brown DN, Wu Z, He F, Miller DJ, Herchenroeder JW. Dysprosium-free melt-spun permanent magnets. *J. Phys.: Condens. Matter.*[J], 2014, 26: 064202.
3. Liu T, Li RY, Zhou L, Shi XN, Wei ZY, Ren M, Guo XY. Progress of coercivity enhancement in sintered NdFeB magnets. *J. Chin. Soc. Rare Earths.*[J], 2024, 1: 1 (in Chin.).
4. Li JN, Sepehri-Amin H, Sasaki T, Ohkubo T, Hono K. Most frequent-ly asked questions about the coercivit y of Nd-Fe-B permanent magnets. *Sci. Technol. Adv. Mater.*[J], 2021, 22(1): 386.
5. Nakamura H, Hirota K, Shimao M. Magnetic properties of extremely small Nd-Fe-B sintered magnets. *IEEE Trans. Magn.*[J], 2005, 41: 3844.
6. Liu ZW, He JY, Zeng CC, Chen SY. Recent progress and future prospect in grain boundary diffusion technology for high performance Nd-Fe-B permanent magnets. *J. Magn. Mater. Devices.*[J], 2023, 54(4): 97.
7. Zhou TJ, Chen J, Wang QR, Pan WM, Huang QF, Liu RH, Li MF, Xie GQ. Super-high coercivity NdFeB magnet fabricated with double Tb-rich/lean shells by double alloy method and grain boundary diffusion. *Journal of Alloys and Compounds.*[J], 2023, 937: 168368.
8. Zhu XD, Wang M, Yu YJ, Wang Q, Wang F, Wang PF, Jia B, Wang C, Zhou B. Coercivity enhancement of sintered Nd-Pr-Fe-B magnets by cost-Effective grain boundary diffusion of Dy/Tb films. *Crystals*[J], 2023, 13: 1516.
9. Sepehri-Amin H, Prabhu D, Hayashi M, Ohkubo T, Hioki K, Hattori A, Hono K. Coercivity enhancement of rapidly solidified Nd-Fe-B magnet powders. *Scr. Mater.*[J], 2013, 68: 167.
10. Lu KC, Bao XQ, Tang MH, Sun L, Li JH, Gao XX. Influence of annealing on microstructural and magnetic properties of Nd-Fe-B magnets by grain boundary diffusion with Pr-Cu and DyCu alloys. *J. Magn. Magn. Mater.*[J], 2017, 441: 517.
11. Zeng HX, Liu ZW, Zhang JS, Liao XF, Yu HY. Towards the diffusion source cost reduction for NdFeB grain boundary diffusion process. *J. Mater. Sci. Technol.*[J], 2020, 36: 50.
12. Zhou Q, Liu ZW, Zhong XC, Zhang GQ. Properties improvement and structural optimization of sintered NdFeB magnets by non-rare earth compound grain boundary diffusion. *Mater. Des.*[J], 2015, 86: 114.
13. Chen W, Huang YL, Luo JM, Hou YH, Ge XJ, Guan YW, Liu ZW, Zhong ZC, Wang GP. Microstructure and improved properties of sintered Nd-Fe-B magnets by grain boundary diffusion of non-rare earth. *J. Magn. Magn. Mater.*[J], 2019, 476: 134.
14. Wang EH, Xiao CH, He JY, Lu CF, Hussain M, Tang RH, Zhou Q, Liu ZW. Grain boundary modification and properties enhancement of sintered Nd-Fe-B magnets by ZnO solid diffusion. *Appl. Surf. Sci.*[J], 2021, 565: 150545.
15. He JY, Liao XF, Lan XX, Qiu WQ, Yu HY, Zhang JS, Fan WB, Zhong XC, Liu ZW. Annealed Al-Cr coating: A hard anti-corrosion coating with grain boundary modification effect for Nd-Fe-B magnets. *J. Alloys Compd.*[J], 2021, 870: 159229.
16. Sepehri-Amin H, Ohkubo T, Gruber M, Schrefl T, Hono K. Micromagnetic simulations on the grain size dependence of coercivity in anisotropic Nd-Fe-B sintered magnets. *Scr. Mater.*[J], 2014, 89: 29.
17. Uestuener K, Katter M, Rodewald W. Dependence of the mean grain size and coercivity of sintered Nd-Fe-B magnets on the initial powder particle size. *IEEE Trans. Magn.* [J],2006, 42(10): 2897.
18. Chen L, Cao XJ, Guo S, Di JH, Ding GF, Yan CJ, Chen RJ, Yan AR. Coercivity enhancement of Dy-free sintered Nd-Fe-B magnets by grain refinement and induction heat treatment. *IEEE Trans. Magn.*[J], 2015, 51(11): 2101403.
19. Guo S, Yang X, Fan X, Ding G, Cao S, Zheng B, Chen R, Yan A. The effect of grain size on the diffusion efficiency and microstructure of sintered Nd-Fe-B magnets by Tb grain boundary diffusion. *Materials*[J], 2022, 15: 4987.
20. Li WF, Ohkubo T, Hono K, Sagawa M. The origin of coercivity decrease in fine grained Nd-Fe-B sintered magnets. *J. Magn. Magn. Mater.*[J], 2009, 321:1100.
21. Cheng XH, Li J, Liu T, Zhou L, Yu XJ, Li B. Effect of Grain size on magnetic properties in grain boundary diffusion NdFeB magnet. *J. Chin. Soc. Rare Earths.*[J], 2020, 38(6): 752.
22. Zhao Changyu, Liu Ying, Zhao Wei, Hou Henan, Li Jun. Effect of Low-Pressure Sintering on Microstructure and Service Stability of NdFeB magnets. *Rare Metal Materials and Engineering*[J], 2023, 52(1): 74~80.
23. Chen K, Zhao HL, Fan FC. Study on the influence of sintered NdFeB substrate composition on grain boundary diffusion. *Rare Metal Materials and Engineering*[J], 2024, 53(3): 841~847.
24. He JY, Yu ZG, Cao JL, Song WY, Xu K, Fan WB, Yu HY, Zhong XC, Mao HY, Mao CY, Liu ZW. Rationally selecting the chemical composition of the Nd-Fe-B magnet for high-efficiency grain boundary diffusion of heavy rare earths. *J. Mater. Chem. C.*[J], 2022, 10: 2080.
25. Xie HZ. Theory and Practice of NdFeB oxygen free process technology[M]. Beijing: Metallurgical Industry Press, 2018. 21 (in Chinese).
26. Zhou TJ, Liu RH, Qu PP, Xie GQ, Li MF, Zhong ZC. Diffusion behavior and coercivity enhancement of Tb-containing NdFeB magnet by dip-coating TbH_3[J]. *J. Mater. Res. Technol.*, 2022, 20: 1391.

27. Liu RH, Qu PP, Zhou TJ, Pan WM, Li MF, Huang QF, Zhong ZC. The diffusion behavior and striking coercivity enhancement by Dip-coating TbH_3 powders in sintered NdFeB magnets[J]. *J. Magn. Magn. Mater.*, 2021, 536: 168091.
28. Luo SG. Effect of grain size on grain boundary diffusion process and properties of sintered NdFeB. Master Thesis, Jiangxi University of Science and Technology[D]. Ganzhou, China, 2022(in Chinese).
29. Ramesh R, Thomas G, Ma BM. Magnetization reversal in nucleation controlled magnets. II. Effect of grain size and size distribution on intrinsic coercivity of Fe-Nd-B magnets[J]. *J. Appl. Phys.*, 1988, 64(11): 6416.

晶粒细化对烧结钕铁硼晶界扩散过程及磁性能的影响

王美[1]， 刘伟明[2]， 彭步庄[3]， 王倩[1]， 王飞[1]， 张玉孟[3]， 顾晓倩[3]， 王 琦[1]， 肖桂勇[1]， 刘艳[3]， 朱新德[1,4]

(1.山东大学材料液固结构演化与加工教育部重点实验室，山东 济南 2500612)
(2. 烟台市标准计量检验检测中心，山东 烟台 264000)
(3. 烟台正海磁性材料有限公司，山东 烟台 264006)
(4. 建新赵氏集团有限公司， 浙江 宁波 315600)

摘要：本文制备了三种成分相同、晶粒尺寸不同的钕铁硼磁体，并在相同的技术参数下使用金属 Tb 进行了晶界扩散。使用 X 射线衍射（XRD）、场发射扫描电子显微镜（FESEM）和电子探针显微分析仪（EPMA）评估扩散过程并对磁体扩散前后的磁性能进行了表征，分析研究了晶粒尺寸对烧结 NdFeB 磁体晶界扩散过程和性能的影响。结果表明，磁体的晶粒细化可以提高 Tb 扩散效率，并使磁体在不同温度下具有更高的矫顽力。这主要是由于在晶界扩散过程中磁体内部形成了更深、更完整的核壳结构，从而使 $Nd_2Fe_{14}B$ 晶粒具有更好的磁隔离和更高的各向异性。这项工作表明细化晶粒可以在低重稀土的情况下提高磁体矫顽力。

关键词：烧结 NdFeB；晶粒细化；晶界扩散；矫顽力

基金项目：山东省重点研发计划（2021CXGC010310）；山东省科技型中小企业创新能力提升项目（2023TSGC0287 和 2024TSGC0519）；山东省自然科学基金 （ZR2022ME222）和国家自然科学基金（51702187）。

通讯作者：朱新德，男，副教授，1982 年生， 博士，山东大学材料液固结构演化与加工教育部重点实验室，山东 济南 250061 和建新赵氏集团有限公司，浙江 宁波 315600，Email：zhuxinde@sdu.edu.cn;
王倩，女，1990 年生，博士，助理研究员，山东大学材料液固结构演化与加工教育部重点实验室，山东 济南 250061，Email：qian.wang@sdu.edu.cn